How to cite: *Angew. Chem. Int. Ed.* **2021**, *60*, 27282–27287
International Edition: doi.org/10.1002/anie.202112764
German Edition: doi.org/10.1002/ange.202112764

Single-Molecule Magnets | Hot Paper

Magnetization Dynamics on Isotope-Isomorphic Holmium Single-Molecule Magnets

Yang Liu[+], Le Tuan Anh Ho[+], Guo-Zhang Huang, Yan-Cong Chen, Liviu Ungur, Jun-Liang Liu,* and Ming-Liang Tong*

Abstract: *Here we reported the deuteration of the metal-binding equatorial water molecules in a reported Ho^{III} single-molecule magnet (SMM) with pentagonal-bipyramidal geometry, from $[Ho(CyPh_2PO)_2(H_2O)_5]^{3+}$ to $[Ho(CyPh_2PO)_2(D_2O)_5]^{3+}$. The hyperfine structures originating from the nuclear spin of $^{165}Ho^{III}$ can be clearly observed. Moreover, the resulting magnetization dynamics revealed the switch of the relative relaxation rates for the two isotope-isomorphic complexes—respectively faster/slower at low/high temperature. The noticeable isotope effect arises from not only the paramagnetic metal center but also the diamagnetic ligands, which can be explained by the ab initio calculated tunnel splitting and the involvement of the super-hyperfine interaction related to the difference in the nuclear spin number of protium (^1H, $I = 1/2$) and deuterium (^2H, $I = 1$).*

Isotope effects reflect the quantum nature of atomic nucleus, which is widely observed and investigated in differing chemical kinetics, solubility, NMR shift, spectroscopy, etc. This topic attracts intense interests from multidiscipline including physics and chemistry.[1–11] Thanks to the considerable mass difference, for example ca. 100 % mass increase from protium (^1H) to deuterium (^2H or D) and the different nuclear spin as well, the isotope effect is more pronounced in further affecting the associated inter/intramolecular behavior, like the strength of hydrogen bond,[12–14] the lattice vibration/spin-phonon coupling,[15–19] and the much smaller gyromagnetic ratio of the deuterium spin (^2H:^1H = 1:6.5). As a weakly interacted monodisperse system, single-molecule magnets (SMMs) exhibit slow magnetic relaxation arising from their large magnetic anisotropy, which shows the ability of magnetic memory at the single-molecule level. Thus, SMMs are regarded as promising candidates for high-density information storage and spintronic devices.[20–27] In fact, they are unlimited to inherently possess magnetization dynamics arising from electronic spin, but potentially collaborate with nuclear spin.[28–32] In terms of the above, isotope effect may regulate the properties of SMMs and bring novel and interesting quantum phenomena.

As far as we know, isotope effects on magnetic relaxation in the research of SMMs are rarely reported.[29–39] Most of them are isotopic enriched or naturally-isotope-pure for the paramagnetic metal centers, like Dy^{III}, Ho^{III}, Er^{III} or Yb^{III} [29–37,40–44] clearly revealing that the nuclear spin of the metal center have significant effects on magnetic behavior. However, magnetization dynamics on the diamagnetic coordination ligands are scarcely studied, only two of which were tried to deuterate the ligand and reported the isotope effects.[38,39] Both cases are transition-metal complexes, while the isotope effects of coordination ligand in lanthanide SMMs, especially for the high-performance Ho^{III} SMMs, still remain phenomenologically ambiguous, let alone the deuterium-driven magnetic relaxation mechanism.

In this context, we focus our attention on a reported Ho^{III} single-ion magnet (SIM),[31] showing quantum effects arising from its nuclear spin on the paramagnetic metal site. Taking notice of the five coordinated water molecules in the equatorial plane, which particularly facilitate the formation of abundant hydrogen bonding networks around Ho^{III} ions, we expect it to be a good model complex to study the magnetic dynamics induced by the protium/deuterium bond from the diamagnetic peripheral ligand. Herein we synthesized the non-deuterated complex $[Ho(CyPh_2PO)_2(H_2O)_5]I_3{\cdot}2(CyPh_2PO){\cdot}2\,EtOH$ (**1**, Cy = cyclohexyl), and the deuterated analog $[Ho(CyPh_2PO)_2(D_2O)_5]I_3{\cdot}2(CyPh_2PO){\cdot}2EtOD$ (**2**). Isotopic substitution from protium to deuterium can be simply implemented in deuterated water and ethanol via active hydrogen exchange. By probing via infrared spectra for **1** and **2**, it clearly reveals that the deuteration is successfully achieved (Figure S1).[10,45,46]

The crystallographic structures were investigated by single-crystal X-ray diffraction (Figure 1, Figure 2a and Table S1). The isostructural **1** and **2** are both crystallized in orthorhombic space group $C222_1$ with the crystallographic C_2 axis passing through the Ho1-O1W. The complete molecular structure is almost identical to the reported one,[31] with two coordinated $CyPh_2PO$ ligands in the axial positions and five coordinated water molecules in the equatorial plane, two uncoordinated $CyPh_2PO$ ligands, three iodide anions and two ethanol molecules.

As depicted, the coordination environment of the Ho^{III} can be regarded as a compressed pentagonal bipyramid. With minor different bond length and bond angle of both complexes, axial Ho–O bonds of 2.202 Å for **1** and 2.196 Å

[*] Dr. Y. Liu,[+] G.-Z. Huang, Dr. Y.-C. Chen, Dr. J.-L. Liu, Prof. Dr. M.-L. Tong
Key Lab of Bioinorganic and Synthetic Chemistry of Ministry of Education, School of Chemistry, Sun Yat-Sen University
Guangzhou 510006 (P. R. China)
E-mail: liujliang5@mail.sysu.edu.cn
Dr. L. T. A. Ho,[+] Dr. L. Ungur
Department of Chemistry, National University of Singapore
Singapore 117543 (Singapore)
E-mail: chmlu@nus.edu.sg
[+] These authors contributed equally to this work.
Supporting information and the ORCID identification number(s) for the author(s) of this article can be found under: https://doi.org/10.1002/anie.202112764.

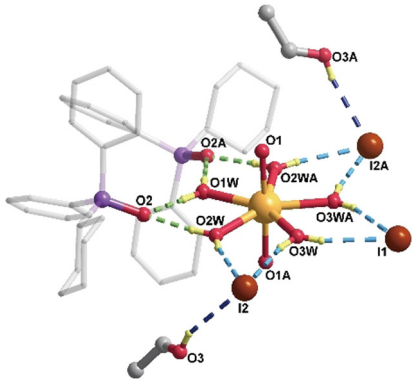

Figure 1. Hydrogen-bonded networks around Ho^{III}. Color codes: Ho, orange; O, red; C, gray; I, brown; P, purple; H, yellow. Symmetry code (A): $-1-x, +y, -1/2-z$.

for **2**, an average equatorial Ho–O bond length of 2.345 Å for **1** and 2.344 Å for **2**. The O1-Ho-O1A bond is very nearly linear, with bond angle of 177.9° for **1** and 177.8° for **2** (Table S2). The values of continuous shape measure (CShM) for coordination geometries of Ho^{III} ion are calculated with SHAPE 2.1 (Table S3),[47,48] which deviates only from the ideal D_{5h} by 0.143 for **1** and 0.149 for **2**, respectively.

Interestingly, compare with the magnetic relaxation time (τ) of both complexes (Figure 2), we found that the ratio in relaxation time (τ_{D_2O}/τ_{H_2O}) becomes greater as the temperature increased (Figure 2d), demonstrating the variation of their magnetic dynamics is strongly temperature dependent. Observed from the χ_M'', the peak significantly shifts from 339 Hz for **1** to 151 Hz for **2** at 20 K, and shifts from 0.79 Hz for **1** to 0.89 Hz for **2** at 7 K (Figure S12). As shown in Figure 2, the τ of the deuterated complex **2** is longer in high temperature region, while the situation reverses <15 K.

As the isotope effect signifies most at ca. 20 K, field-dependent alternating-current (ac) magnetic susceptibilities were carried out for **1** and **2** in order to investigate their fine structures arising from the nuclear spin (Figure 2c, S12–S15). The relaxation times for **2** are all longer than those of **1** at 20 K (Figure 2c), with the oscillation of τ_{D_2O}/τ_{H_2O}. Additionally, τ_{D_2O}/τ_{H_2O} becomes greater at some specific low fields at 0, 0.06, 0.11 and 0.16 T, while smaller than at 0.03, 0.085, 0.13

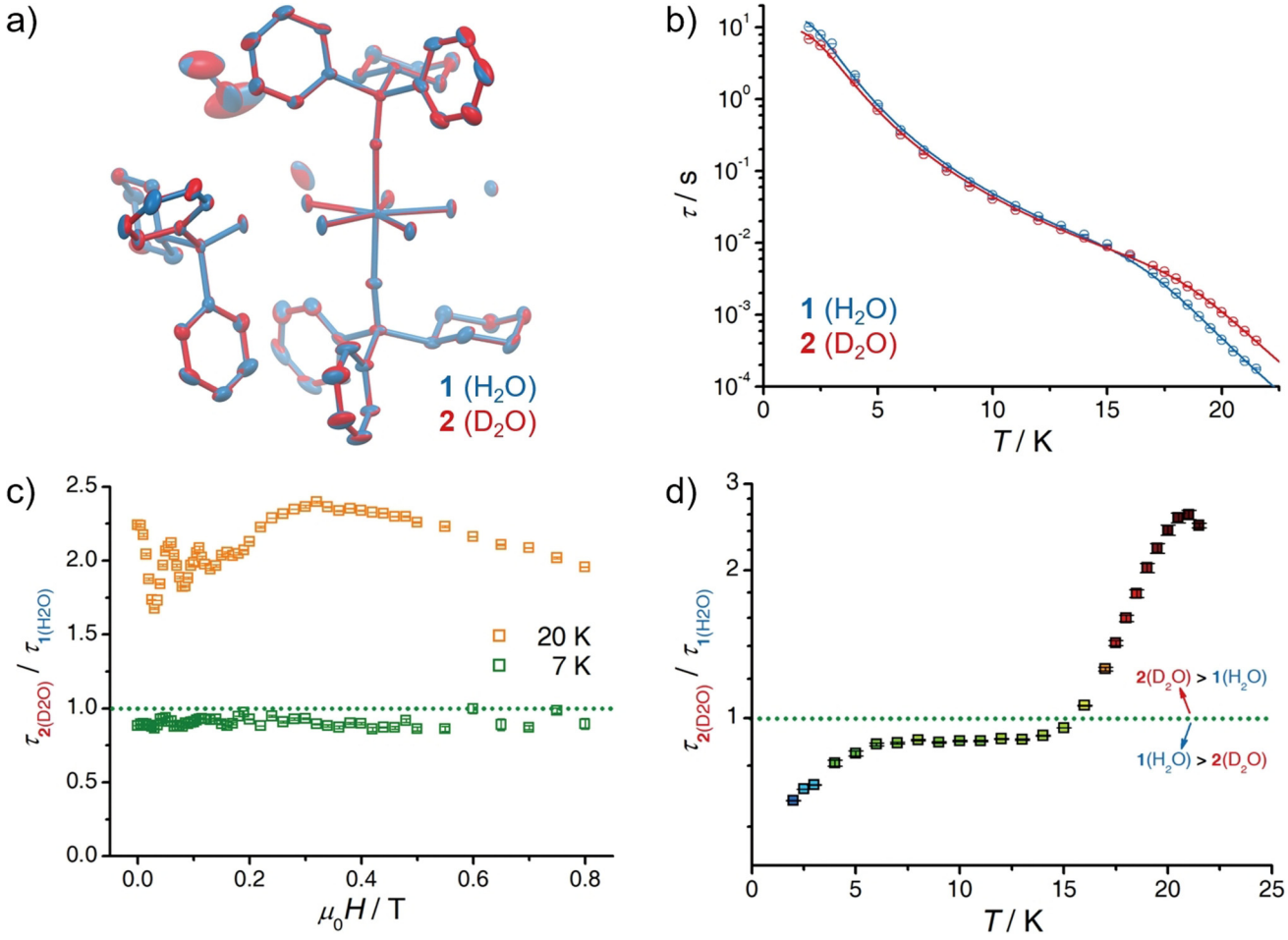

Figure 2. a) Overlapping diagram of structures of **1** (blue) and **2** (red).[58] Hydrogen atoms and the crystallographic-symmetric peripheral parts (one uncoordinated $CyPh_2PO$ ligand, one I^- anion and one ethanol molecule) are omitted for clarity. b) Temperature dependence of relaxation time τ with error bars under zero dc magnetic field for **1** (blue) and **2** (red). The solid lines correspond to the best fits as shown in Figure S11. c) Field dependence of τ_{D_2O}/τ_{H_2O} with error bars at 20 K (yellow) and 7 K (green). d) Temperature dependence of τ_{D_2O}/τ_{H_2O} with error bars under zero dc magnetic field.

and 0.17 T, with a period of approximately 0.06 T (Figure 2c). In contrast, such isotope effect virtually vanishes at low temperature as it is demonstrated at 7 K (Figure 2c). This appearance and disappearance of the oscillation in the field-dependent τ_{D_2O}/τ_{H_2O} at different temperatures between two isomorphic complexes emphasizes more the difference in magnetization dynamics due to the isotope effect.

These strongly temperature- and field-dependent divergences denote the isotope effect from the deuteration of the complex. As far as we are aware, these phenomena have not been observed and explained so far.

For further insight into the isotope effect on magnetic anisotropy of the complexes, CASSCF/RASSI/SINGLE_ANISO type calculations were performed using OpenMOLCAS program.[49–55] For this purpose, we employed the $[Ho(CyPh_2PO)_2(H_2O)_5]I_3$ unit for **1** and $[Ho(CyPh_2PO)_2(D_2O)_5]I_3$ for **2**. Three I^- and two $CyPh_2PO$ were also included in the calculation explicitly. The obtained ab initio results are given in Table S4. As expected, the energy separation is in line with previously published Ho^{III} in similar D_{5h}-environment, offering quite good magnetic axiality for Ho and Dy elements.[31,56,57]

Relaxation of a coordinated complex strongly depends on its energy spectrum. For both complexes, the strong anisotropic effect on the Ho^{III} metal ion induces a large energy gap between the ground and excited doublets at over 200 cm^{-1} (Table S4 and Figure 3a), which is relatively high comparing to the temperature where magnetic dynamics is measured (up to around 20 K). Further hyperfine interaction between the Ho^{III} nuclear spin $I = {}^7/_2$ and its electron spins splits each electronic doublet into multiple multiplets of 16 hyperfine-electronic energy levels (Figure 3b). This hyperfine splitting has a huge effect in blocking the quantum tunneling of magnetization, which effectively make this channel be the bottleneck of magnetization relaxation on the whole investigated temperature range.[32] Observations of the oscillations in the field-dependent τ (Figure S15) indeed confirm this conclusion.

Experimental data for the period of the oscillation in the field-dependent τ at both 7 K and 20 K for both complexes also allow us to extract a corresponding hyperfine constant around $g\mu_B\Delta B \approx 0.35$ cm^{-1} where $\Delta B \approx 60$ mT is the period at low applied magnetic field (Figure S15). The fact that there is no isotope effect to the hyperfine coupling, which is

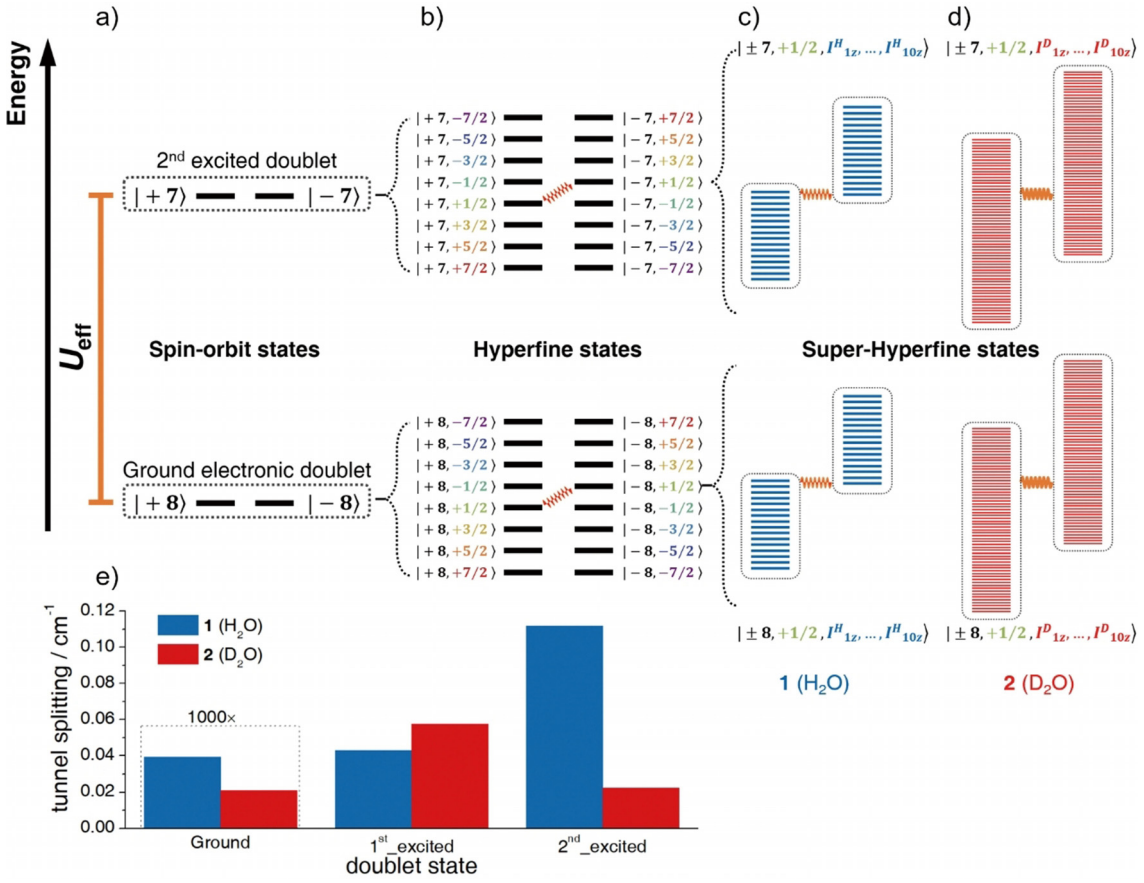

Figure 3. Energy spectrum where the relaxation occurs a) Electronic energy splitting under the ligand field. b) Hyperfine splitting due to the coupling between the nuclear and electronic spin of Ho^{III}. At zero field, quantum tunneling of the magnetization can only take place between localized states with the same nuclear spin I_z of Ho^{III}. c) and d) Super-hyperfine splitting of each hyperfine-electronic state, which effectively broadens the quantum tunneling window and is the key in differentiating magnetization dynamics between two isotope-isomorphic **1** (c) and **2** (d). Here U_{eff} denotes the effective blocking barrier. Wavy lines in c) and d) stand for the bottleneck of the relaxation process, the quantum tunneling of magnetization. This schematic relaxation energy spectrum is valid for both **1** and **2**. e) The comparison of tunnel splitting of the 3 low-lying electronic doublet states from ab initio calculations for **1** (red) and **2** (blue).

manifested as the same oscillation period for **1** and **2**, is reasonable considering that the nucleus and electrons of the metal ion is much closer than the water/heavy water ring and the metal ion. The same oscillation period, and accordingly the hyperfine constant, in both complexes indicates that the hyperfine-splitting of the electronic ground doublet in **1** and **2** are the same in experiment (Figure 3b).

Due to the close distance and bonding between five coordinated water/heavy water molecules with the centered metal ion, super-hyperfine interaction between $^{1}H/^{2}H$ nuclear spin and the electron spin of Ho^{III} is facilitated, which then further splits each hyperfine-electronic state into practically a band of a width proportional to the super-hyperfine constant and $^{1}H/^{2}H$ nuclear spin number. This effectively broadens the magnetization quantum tunneling windows (Figure 3c,d) and eases the relaxation via quantum tunneling channel.

At low temperature, relaxation of magnetization mainly occurs within the lowest multiplet corresponding to the ground non-Kramers electronic doublet. Besides the Raman process, quantum tunneling process in this temperature domain and at zero external field basically depends on 1) the tunnel splitting of the ground non-Kramers electronic doublet resulting from the ligand field (Figure 3e, Table S4); 2) the probability of the fluctuation of the internal dipolar field to shift the energy spectrum into resonance 3) the amount of overlap of the energy bands having the same metal ion nuclear spin projection along the easy axis (z-axis) but opposite electronic magnetic moment; 4) the density of states within a band. Ab initio calculation (see SI) shows that tunnel splitting of the ground electronic doublet of **1** is 1.87 times larger than **2**, which usually leads to a faster relaxation in **1**.

However, the key factor in relaxation of **1** and **2** at low temperature, in fact, results from the super-hyperfine interaction. Supposing that the super-hyperfine interaction in both complexes is the same since there is no large difference in molecular structure. The fact that the nuclear spin number of ^{2}H ($I=1$) is twice larger than one of ^{1}H ($I=^{1}/_{2}$) not only gives rise to a super-hyperfine band width twice larger in energy spectrum of **2** than **1** ($\mathcal{H}_{shf} \approx A_{shf}\tilde{S}_z I_z$), but also generates a much denser density of super-hyperfine-split states for the former, ca. $(2I+1)^n$ where n is the number of hydrogen nuclear spins. Consequently, under the same fluctuation of the internal dipolar field, it is easier to shift hyperfine-split states of **2** into resonance than **1**. The denser density also helps counteracts the effect of a slightly larger tunnel splitting in **1**. As a results, relaxation in **1** is still slower than **2** at low temperature as observed in Figure 2.

The above situation changes substantially at high temperature when the magnetization relaxation involves the excited doublets. Ab initio calculations of the transition magnetic moment show that before transiting via the quantum tunneling channel, the dominant relaxation should be first from the ground doublet to the 2nd excited doublet, which is at 233 cm^{-1} for **1** and 236 cm^{-1} for **2** (Table S4, Figure S16), which are in very good agreement with the fitted effective blocking barriers for both complexes obtained from experiment (233.5 cm^{-1} and 248 cm^{-1}, Figure S11). After transition to this 2nd excited doublet, due to hyperfine splitting of the electronic structure, bottleneck of the relaxation is still the population transition via quantum tunneling between states with opposite electronic magnetic moment (left and right hand side of the energy spectrum in Figure 3b,c,d).[31] State-of-the-art ab initio data shows that, different from the ground electronic doublet, tunnel splitting within this non-Kramers 2nd-excited electronic doublet of **1** is about 5 times larger than **2** (Table S4, Figure 3e, S16), which should then dominates the counter-effect from the bandwidth broadening and high density of states due to the larger nuclear spin number of ^{2}H in **2**. This clearly results in a significantly faster relaxation in the former, which leads to the observed large ratio τ_{D_2O}/τ_{H_2O} at high temperature domain.

As observed from the experiment, another unusual feature showing the isotope effect comes from the field-dependent τ_{D_2O}/τ_{H_2O} at 7 K and 20 K (Figure 2c). In fact, this is just a confirmation about the difference in relaxation mechanism at low and high temperature as well as the involvement of the super-hyperfine interaction in further splitting the energy spectrum. As investigated previously,[31,32] the positive peaks of field-dependent τ are originated from the hyperfine-electronic energy levels crossings while the negative peaks are from levels avoided-crossings (Figure S15). Additionally, it was also demonstrated that the damping of the oscillation in the field-dependent τ (Figure S15) in systems with hyperfine interaction is merely a consequence of the random orientation of the molecules in the polycrystalline sample and accordingly the relaxation profile (relaxation rate of a single-crystal sample in the vicinity of the level crossings/anti-crossings and the domain between crossing and anti-crossing).

Comparing to lower temperature range, at 7 K, due to the involvement of relaxation via excited electronic doublets, which leads to a faster rate in **1** vs. **2**, to compensate the quantum tunneling window broadening effect in the ground doublet, which is stronger in **2** vs. **1**, field dependence of the τ for both complexes is similar (Figure 2b, S15a) and so is their ratio (around unity, see Figure 2c). In other words, relaxation profiles of both system **1** and **2** at 7 K are quite similar.

On the contrary, relaxation profiles at 20 K are significantly different as quantum tunneling rate in **1** is much faster than **2** as explained. The difference in the relaxation profiles of two isotopes at different temperature is due to the super-hyperfine interaction involvement and the tunnel splittings, together with the oscillation of the time-dependent τ due to the hyperfine interaction, then resulting in the observed damping oscillation in τ_{D_2O}/τ_{H_2O} as well. This can be validated using the simple model developed in the previous work.[31,32] Our numerical calculation using this (SI, Section 6) indeed confirms that τ_{D_2O}/τ_{H_2O} oscillation is magnified due to this difference in the field-dependent relaxation profiles, which is nothing but a manifestation of the discussed isotope effect on the energy spectrum of **1** and **2**.

As for the smaller gyromagnetic ratio for ^{2}H vs. ^{1}H, thus reducing the nuclear magnetic moment, is not so important in this case. In both complexes, the bonding between the water ring and the Ho^{III} is strong, making the contact effect (mainly the super-exchange origin) much stronger than the dipolar

one and we have to split the energy spectrum to super-hyperfine level to explain the relaxation. In the opposite case that the contact effect is weaker than the dipolar one, an internal field is a good approximation, accordingly phenomenon similar to the isotopic Fe_8 may be found.[23,38]

In conclusion, we replaced the coordination water in the equatorial plane of complex $[Ho(CyPh_2PO)_2(H_2O)_5]I_3{\cdot}2(CyPh_2PO){\cdot}2EtOH$ (**1**) with deuterium water by isotope substitution, then we got the isotope-isomorphic complex $[Ho(CyPh_2PO)_2(D_2O)_5]I_3{\cdot}2(CyPh_2PO){\cdot}2EtOD$ (**2**). Ultimately, experimental magnetization dynamics investigation shows that the temperature-dependent relaxation time of **1** is longer below 15 K, while the opposite situation happens above 15 K. This unobserved phenomenon is amplified in field-dependent relaxation times ratio at different temperature. Based on ab initio calculations, the difference between the magnetization relaxation and its mechanism within these isotopic complexes has been elucidated. Indeed, our theoretical analysis points out that despite similar molecular structure as they are, the involvement of the super-hyperfine interaction and the difference in the nuclear spin number of protium ($I = {}^1/_2$) and deuterium ($I = 1$) plays an important role in forming superhyperfine-hyperfine-electronic energy spectrum, which accordingly leads to differences in the magnetization dynamics of these two isotopic-isomorphic complexes.

Acknowledgements

This work was supported by the National Key Research and Development Program of China (2018YFA0306001), the NSFC (Grant nos 21620102002, 21822508, 22073115 and 21821003), and the Pearl River Talent Plan of Guangdong (2017BT01C161). L.U. acknowledges the financial support of the research projects R-143-000-A65-133, R-143-000-A80-114 and R-143-000-B80-114 of the National University of Singapore. Ab initio calculations were done on the ASPIRE-1 cluster (http://www.nscc.sg) under the project 11001278. J.L.L. also thanks Dr. Kasper S. Pedersen from Technical University of Denmark for his inspiring and valuable suggestion.

Conflict of Interest

The authors declare no conflict of interest.

Keywords: hyperfine interaction · isotope effect · magnetization dynamics · single-molecule magnets · super-hyperfine interaction

[1] S. Crawford, M. T. Kirchner, D. Bläser, R. Boese, W. I. F. David, A. Dawson, A. Gehrke, R. M. Ibberson, W. G. Marshall, S. Parsons, O. Yamamuro, *Angew. Chem. Int. Ed.* **2009**, *48*, 755 – 757; *Angew. Chem.* **2009**, *121*, 769 – 771.
[2] T. G. Gant, *J. Med. Chem.* **2014**, *57*, 3595 – 3611.
[3] C. Shi, X. Zhang, C.-H. Yu, Y.-F. Yao, W. Zhang, *Nat. Commun.* **2018**, *9*, 481.
[4] G. Hummer, S. Garde, A. E. García, L. R. Pratt, *Chem. Phys.* **2000**, *258*, 349 – 370.
[5] E. Sabadini, T. Cosgrove, F. do Carmo Egídio, *Carbohydr. Res.* **2006**, *341*, 270 – 274.
[6] R. Lässer, K. H. Klatt, *Phys. Rev. B* **1983**, *28*, 748 – 758.
[7] M. Kainosho, T. Torizawa, Y. Iwashita, T. Terauchi, A. Mei Ono, P. Güntert, *Nature* **2006**, *440*, 52 – 57.
[8] H. Benedict, H.-H. Limbach, M. Wehlan, W.-P. Fehlhammer, N. S. Golubev, R. Janoschek, *J. Am. Chem. Soc.* **1998**, *120*, 2939 – 2950.
[9] C. L. Perrin, A. Shrinidhi, K. D. Burke, *J. Am. Chem. Soc.* **2019**, *141*, 17278 – 17286.
[10] Y. Zhang, W. Zhang, S.-H. Li, Q. Ye, H.-L. Cai, F. Deng, R.-G. Xiong, S. D. Huang, *J. Am. Chem. Soc.* **2012**, *134*, 11044 – 11049.
[11] S. Koval, J. Kohanoff, J. Lasave, G. Colizzi, R. L. Migoni, *Phys. Rev. B* **2005**, *71*, 184102.
[12] S. Scheiner, M. Čuma, *J. Am. Chem. Soc.* **1996**, *118*, 1511 – 1521.
[13] G. A. Jeffrey, *An Introduction to Hydrogen Bond*, Oxford University Press, New York, **1997**.
[14] C. N. R. Rao, *J. Chem. Soc. Faraday Trans. 1* **1975**, *71*, 980 – 983.
[15] J. R. Durig, S. M. Craven, K. K. Lau, J. Bragin, *J. Chem. Phys.* **1971**, *54*, 479 – 487.
[16] A. B. Harris, *Phys. Rev. B* **1970**, *2*, 3495 – 3525.
[17] G. Taddei, H. Bonadeo, M. P. Marzocchi, S. Califano, *J. Chem. Phys.* **1973**, *58*, 966 – 978.
[18] G. J. Kearley, M. R. Johnson, J. Tomkinson, *J. Chem. Phys.* **2006**, *124*, 044514.
[19] D. H. Moseley, S. E. Stavretis, K. Thirunavukkuarasu, M. Ozerov, Y. Cheng, L. L. Daemen, J. Ludwig, Z. Lu, D. Smirnov, C. M. Brown, A. Pandey, A. J. Ramirez-Cuesta, A. C. Lamb, M. Atanasov, E. Bill, F. Neese, Z.-L. Xue, *Nat. Commun.* **2018**, *9*, 2572.
[20] R. Sessoli, D. Gatteschi, A. Caneschi, M. A. Novak, *Nature* **1993**, *365*, 141 – 143.
[21] M. N. Leuenberger, D. Loss, *Nature* **2001**, *410*, 789 – 793.
[22] N. Ishikawa, M. Sugita, T. Ishikawa, S.-y. Koshihara, Y. Kaizu, *J. Am. Chem. Soc.* **2003**, *125*, 8694 – 8695.
[23] D. Gatteschi, R. Sessoli, J. Villain, *Molecular nanomagnets*, *Vol. 9*, Oxford University Press, New York, **2006**.
[24] L. Bogani, W. Wernsdorfer, *Nat. Mater.* **2008**, *7*, 179 – 186.
[25] F. Troiani, M. Affronte, *Chem. Soc. Rev.* **2011**, *40*, 3119 – 3129.
[26] S. Thiele, F. Balestro, R. Ballou, S. Klyatskaya, M. Ruben, W. Wernsdorfer, *Science* **2014**, *344*, 1135 – 1138.
[27] F.-S. Guo, B. M. Day, Y.-C. Chen, M.-L. Tong, A. Mansikkamäki, R. A. Layfield, *Science* **2018**, *362*, 1400 – 1403.
[28] W. Wernsdorfer, M. Ruben, *Adv. Mater.* **2019**, *31*, 1806687.
[29] F. Pointillart, K. Bernot, S. Golhen, B. Le Guennic, T. Guizouarn, L. Ouahab, O. Cador, *Angew. Chem. Int. Ed.* **2015**, *54*, 1504 – 1507; *Angew. Chem.* **2015**, *127*, 1524 – 1527.
[30] N. Ishikawa, M. Sugita, W. Wernsdorfer, *J. Am. Chem. Soc.* **2005**, *127*, 3650 – 3651.
[31] Y.-C. Chen, J.-L. Liu, W. Wernsdorfer, D. Liu, L. F. Chibotaru, X.-M. Chen, M.-L. Tong, *Angew. Chem. Int. Ed.* **2017**, *56*, 4996 – 5000; *Angew. Chem.* **2017**, *129*, 5078 – 5082.
[32] S.-G. Wu, Z.-Y. Ruan, G.-Z. Huang, J.-Y. Zheng, V. Vieru, G. Taran, J. Wang, Y.-C. Chen, J.-L. Liu, L. T. A. Ho, L. F. Chibotaru, W. Wernsdorfer, X.-M. Chen, M.-L. Tong, *Chem* **2021**, *7*, 982 – 992.
[33] Y. Kishi, F. Pointillart, B. Lefeuvre, F. Riobé, B. Le Guennic, S. Golhen, O. Cador, O. Maury, H. Fujiwara, L. Ouahab, *Chem. Commun.* **2017**, *53*, 3575 – 3578.
[34] J. Flores González, F. Pointillart, O. Cador, *Inorg. Chem. Front.* **2019**, *6*, 1081 – 1086.
[35] E. Moreno-Pineda, M. Damjanović, O. Fuhr, W. Wernsdorfer, M. Ruben, *Angew. Chem. Int. Ed.* **2017**, *56*, 9915 – 9919; *Angew. Chem.* **2017**, *129*, 10047 – 10051.

[36] L. Scherthan, S. F. M. Schmidt, H. Auerbach, T. Hochdörffer, J. A. Wolny, W. Bi, J. Zhao, M. Y. Hu, T. Toellner, E. E. Alp, D. E. Brown, C. E. Anson, A. K. Powell, V. Schünemann, *Angew. Chem. Int. Ed.* **2019**, *58*, 3444 – 3449; *Angew. Chem.* **2019**, *131*, 3482 – 3487.
[37] L. Scherthan, R. F. Pfleger, H. Auerbach, T. Hochdörffer, J. A. Wolny, W. Bi, J. Zhao, M. Y. Hu, E. E. Alp, C. E. Anson, R. Diller, A. K. Powell, V. Schünemann, *Angew. Chem. Int. Ed.* **2020**, *59*, 8818 – 8822; *Angew. Chem.* **2020**, *132*, 8902 – 8907.
[38] W. Wernsdorfer, A. Caneschi, R. Sessoli, D. Gatteschi, A. Cornia, V. Villar, C. Paulsen, *Phys. Rev. Lett.* **2000**, *84*, 2965 – 2968.
[39] J. Li, S.-J. Xiong, C. Li, B. Jin, Y.-Q. Zhang, S.-D. Jiang, Z.-W. Ouyang, Z. Wang, X.-L. Wu, J. van Tol, Y. Song, *CCS Chem.* **2020**, *2*, 2548 – 2556.
[40] F. Luis, M. J. Martínez-Pérez, O. Montero, E. Coronado, S. Cardona-Serra, C. Martí-Gastaldo, J. M. Clemente-Juan, J. Sesé, D. Drung, T. Schurig, *Phys. Rev. B* **2010**, *82*, 060403.
[41] E. Moreno-Pineda, G. Taran, W. Wernsdorfer, M. Ruben, *Chem. Sci.* **2019**, *10*, 5138 – 5145.
[42] J. Flores González, H. Douib, B. Le Guennic, F. Pointillart, O. Cador, *Inorg. Chem.* **2021**, *60*, 540 – 544.
[43] J. Flores González, B. Lefeuvre, B. Degraeve, O. Cador, F. Pointillart, *Dalton Trans.* **2021**, *50*, 11466 – 11471.
[44] F. Ortu, D. Reta, Y.-S. Ding, C. A. P. Goodwin, M. P. Gregson, E. J. L. McInnes, R. E. P. Winpenny, Y.-Z. Zheng, S. T. Liddle, D. P. Mills, N. F. Chilton, *Dalton Trans.* **2019**, *48*, 8541 – 8545.
[45] R. Bandyopadhyay, J. H. Nguyen, A. Swidan, C. L. B. Macdonald, *Angew. Chem. Int. Ed.* **2013**, *52*, 3469 – 3472; *Angew. Chem.* **2013**, *125*, 3553 – 3556.
[46] M. R. Pedrosa, J. Escribano, R. Aguado, V. Díez, R. Sanz, F. J. Arnáiz, *Polyhedron* **2007**, *26*, 3695 – 3702.
[47] S. Alvarez, P. Alemany, D. Casanova, J. Cirera, M. Llunell, D. Avnir, *Coord. Chem. Rev.* **2005**, *249*, 1693 – 1708.
[48] D. Casanova, M. Llunell, P. Alemany, S. Alvarez, *Chem. Eur. J.* **2005**, *11*, 1479 – 1494.
[49] F. Aquilante, J. Autschbach, R. K. Carlson, L. F. Chibotaru, M. G. Delcey, L. De Vico, I. Fdez. Galván, N. Ferré, L. M. Frutos, L. Gagliardi, M. Garavelli, A. Giussani, C. E. Hoyer, G. Li Manni, H. Lischka, D. Ma, P. Å. Malmqvist, T. Müller, A. Nenov, M. Olivucci, T. B. Pedersen, D. Peng, F. Plasser, B. Pritchard, M. Reiher, I. Rivalta, I. Schapiro, J. Segarra-Martí, M. Stenrup, D. G. Truhlar, L. Ungur, A. Valentini, S. Vancoillie, V. Veryazov, V. P. Vysotskiy, O. Weingart, F. Zapata, R. Lindh, *J. Comput. Chem.* **2016**, *37*, 506 – 541.
[50] B. O. Roos, R. Lindh, P.-Å. Malmqvist, V. Veryazov, P.-O. Widmark, *J. Phys. Chem. A* **2005**, *109*, 6575 – 6579.
[51] B. A. Heß, C. M. Marian, U. Wahlgren, O. Gropen, *Chem. Phys. Lett.* **1996**, *251*, 365 – 371.
[52] F. Aquilante, P.-Å. Malmqvist, T. B. Pedersen, A. Ghosh, B. O. Roos, *J. Chem. Theory Comput.* **2008**, *4*, 694 – 702.
[53] P. Å. Malmqvist, B. O. Roos, B. Schimmelpfennig, *Chem. Phys. Lett.* **2002**, *357*, 230 – 240.
[54] L. F. Chibotaru, L. Ungur, *J. Chem. Phys.* **2012**, *137*, 064112.
[55] L. Ungur, L. F. Chibotaru, *Chem. Eur. J.* **2017**, *23*, 3708 – 3718.
[56] J.-L. Liu, Y.-C. Chen, M.-L. Tong, *Chem. Soc. Rev.* **2018**, *47*, 2431 – 2453.
[57] L. Ungur, L. F. Chibotaru, *Inorg. Chem.* **2016**, *55*, 10043 – 10056.
[58] Deposition Numbers 2110632 (for **1**) and 2110633 (for **2**) contain the supplementary crystallographic data for this paper. These data are provided free of charge by the joint Cambridge Crystallographic Data Centre and Fachinformationszentrum Karlsruhe Access Structures service www.ccdc.cam.ac.uk/structures.

Manuscript received: September 19, 2021
Revised manuscript received: October 16, 2021
Accepted manuscript online: October 20, 2021
Version of record online: November 10, 2021

